Topological Analysis of Electron Density in Depleted Homopolar Chemical Bonds

ROSA LLUSAR,[1] ARMANDO BELTRÁN,[1] JUAN ANDRÉS,[1] STÉPHANE NOURY,[2] BERNARD SILVI[2]

[1]*Departament de Ciències Experimentals, Universitat Jaume I, Box 224, 12080 Castelló, Spain*
[2]*Laboratoire de Chimie Théorique, Université Pierre et Marie Curie, UMR-CNRS 7616, Paris, France*

Received 30 March 1999; accepted 22 May 1999

ABSTRACT: Except for the case of van der Waals interactions, homopolar bonds are covalent and therefore a concentration of the electron density is expected at the bond midpoint. Many experimental and theoretical studies have reported standard deformation density maps and molecular density minus spherical atoms densities, which show a depletion of electron density between formally covalently bonded atoms. For example, electron deficits are found in the theoretical map of the F—F bond in F_2, in the experimental map of the N—N bond in carbonohydrazide, and in the experimental and theoretical maps of the O—O bond in 1,2,7,8-tetraaza-4,5,10,11-tetraoxatricyclo[6.4.1.1]tetradecane. Other partitioning schemes, such as subtraction of valence state atoms rather than spherical atoms from the total density, have been proposed to interpret these unexpected features. In the present work we examine these electronically depleted covalent bonds on the basis of the topological analysis of the electron localization function (ELF) of theoretically calculated electron densities. The attractors of ELF determine basins that are either core or valence basins. The valence basins are characterized by the number of core basins with which they share a common boundary, and this number is called the synaptic order. Disynaptic valence basins have been found for the F—F bond in F_2, for the N—N bond in carbonohydrazide and for the O—O bond in 1,2,7,8-tetraaza-4,5,10,11-tetraoxatricyclo[6.4.1.1]tetradecane. In the case of F_2, polarization functions increase the V(F, F′) basin population, whereas accounting for the Coulomb correlation lowers this basin population. The results calculated for F_2 are compared with those obtained for other diatomic molecules, such as N_2 and O_2, and the ELF picture of the bond compared with the molecular orbital analysis. In the case of carbonohydrazyde, the V(N, N′) basin population is the lowest among all the populations of the disynaptic valence basins present in the molecule, in good agreement with the experimental observations. Analogous results are

Correspondence to: R. Llusar; email: llusar@exp.uji.es
Contract/grant sponsor: Ministerio de Educación y Ciencia of Spain; contract/grant number: PB96-0795-C02-022
Contract/grant sponsor: Consellerría de Educación y Ciencia de la Generalitat Valenciana

CCC 0192-8651 / 99 / 141517-10

obtained for the V(O, O′) basin population in 1,2,7,8-tetraaza-4,5,10,11-tetraoxatricyclo[6.4.1.1]tetradecane. Population fluctuation analysis indicates a strong delocalization of the electron density toward lone pairs and adjacent bonds. © 1999 John Wiley & Sons, Inc. J Comput Chem 20: 1517–1526, 1999

Keywords: electron localization function; depleted homopolar chemical bond; second row homonuclear diatomic molecules; carbonohydrazide; 1,2,7,8-tetraaza-4,5,10,11-tetraoxatricyclo[6.4.1.1]tetradecane

Introduction

Homopolar bonds in neutral systems, except for van der Waals interactions such as in noble gas dimers, are unambiguously covalent, regardless of the definition of a covalent bond. There is a general belief which considers that covalent bonds are formed as a result of the buildup of charge in the internuclear region via an overlap of the relevant atomic wave functions. In the case of H_2^+, the application of the virial theorem to the bonding and antibonding states of the molecule shows that the bond is formed via a lowering of the potential energy as a result of the increase in charge between the nuclei.[1] Based on this idea the obvious way to analyze a chemical bond is through calculated or experimentally measured electron densities. However, there are many problems from both the experimental and the theoretical points of view.[2, 3] Most experimental studies measure what is called the standard deformation density, $\Delta\rho(\mathbf{r})$, which is defined as the molecular electron density, directly obtained form x-ray diffraction data, minus the electron density of the promolecule made up of the superposition of isolated, neutral, spherically averaged, ground state atoms. The experimental maps of various organic molecules show weak bonding density accumulations for NN, CN, CO, and CF bonds. For example, electron density deformation maps obtained from an accurate low-temperature analysis of 1,2,7,8-tetraaza-4,5,10,11-tetraoxotricyclo[6.4.1.1]tetradecane show a density deficit at the center of the OO bond and only weak density accumulations at the center of the CO and NN bonds.[4] A depletion of electron density in NN bonds has previously been noted from studies of *N′N* diformylhydracine and carbonohydrazide.[5, 6]

On the other hand, the deformation density observed for the OO bond is similar to that calculated for the F_2 molecule when the computed difference maps are based on subtraction of spherically averaged densities for F atoms in their ground state. However, the use of spherically averaged ground state charge densities for the atoms constituting the promolecule has been questioned because it does not take into account the hybridization at each atom as "it prepares itself" for bonding.[7] In the case of the F_2 molecule, subtraction of the electron densities of optimally hybridized valence-state F atoms reveals not only the accumulation of charge in the internuclear region but also the concomitant depletion of charge in the nonbonding regions beyond the nuclear centers, which together are the characteristics of the covalent bond. The appearance of a deformation density depends crucially on the definition of the reference state used in its calculation. This has occasionally been interpreted as an ambiguity against the use of deformation density as an analytical tool. In our opinion, a deformation density is meaningful only in terms of its reference state, which must be taken into account in the interpretation. The different deformation functions are complementary and, when used properly, they provide a detailed understanding of the steps involved in the bond formation process.[8]

Bader and coworkers analyzed the total density by examining the electron density, $\rho(\mathbf{r})$, and its Laplacian, $\nabla^2\rho(\mathbf{r})$. Topological analysis of the total density has a considerable advantage over the use of the deformation densities in that it is reference-state-independent. In Bader's analysis of the electron density a shared interaction (i.e., a covalent bond or a dative bond) was characterized by a rather large value of the charge density $\rho(\mathbf{r}_c)$ at the bond critical point and by a negative value of the Laplacian $\nabla^2\rho(\mathbf{r})_{\mathbf{r}=\mathbf{r}_c}$. On the other hand, a closed-shell interaction presents a low $\rho(\mathbf{r}_c)$ value at the bond critical point and positive values of the Laplacian, $\nabla^2\rho(\mathbf{r})_{\mathbf{r}=\mathbf{r}_c}$. These two complementary criteria are related to the same physical idea, namely, in a covalent bond there is a concentration of electron density in the internuclear region. For F_2, $\nabla^2\rho(\mathbf{r})_{\mathbf{r}=\mathbf{r}_c}$ is small or slightly negative (for correlated wave functions) and the Laplacian distribution of $\rho(\mathbf{r})$ is intermediate between the shared and closed-shell interaction limits.

In fact, covalent and dative bonds, according to the Lewis approach, require the sharing of an electron pair rather than a charge concentration. The criteria, based on an analysis of the charge density, are too restrictive to account for the wide spectra of covalent and dative bonds.

Another possibility for analysis of chemical bonds is through energetic considerations related to the compelling interplay of changes in the potential and kinetic energies. This can be done by applying the local expression of the virial theorem to the critical point, derived by Bader, $\frac{1}{2}\nabla^2\rho(\mathbf{r}) = 2G(\mathbf{r}) + V(\mathbf{r})$, where $G(\mathbf{r})$ and $V(\mathbf{r})$ are the kinetic and potential energy densities, respectively.[9] Cremer and Kraka demonstrated that the sign of the total energy density, $H(\mathbf{r})$, where $H(\mathbf{r}) = G(\mathbf{r}) + V(\mathbf{r})$, is an index of the amount of covalency in the chemical interaction.[10] The covalent bond condition, $H(\mathbf{r}_c) < 0$, holds for F_2, even when the calculated value for $\nabla^2\rho(\mathbf{r}_c)_{\mathbf{r}=\mathbf{r}_c}$ is positive.[11] This study shows that, in spite of the density flow out of the internuclear region upon F—F bond formation, the residual density is sufficient to contribute to bond stabilization via an increase in $|V(\mathbf{r})|$.

Recently, Krokidis et al.[12] proposed a rigorous definition of covalent versus dative bonds within a mathematical model, which recovers most features of the Lewis approach. This approach is based on the topological analysis of the Becke and Edgecombe electron localization function (ELF),[13] which enables a partitioning of the molecular space into regions corresponding to the core, bonds, and lone pairs. These analysis considers not only the topological properties of the equilibrium structure but, overall, the evolution of the bonding along the paths yielding bond dissociations or bond formations.

The purpose of this work is to examine, on the basis of the topological analysis of ELF, the bond in molecules for which an electron deficit has been pointed out such as the F—F bond in F_2, the N—N bond in carbonohydrazide (CH_6N_4O) and the O—O bond in 1,2,7,8-tetraaza-4,5,10,11-tetraoxatricyclo[6.4.1.1]tetradecane ($C_6H_{12}N_4O_4$). The bonding in other diatomic molecules, such as N_2 and O_2, has also been analyzed for purposes of comparison.

Topological Analysis of ELF Function

The electron localization function (ELF), introduced by Becke and Edgecombe,[13] is a local function, that describes how efficient the Pauli repulsion is at a given point in the molecular space. In the seminal work of Becke and Edgecombe, ELF was derived from the Laplacian of the conditional probability, $\nabla^2 P_{cond}(\mathbf{r}_1, \mathbf{r}_2)_{\mathbf{r}_1=\mathbf{r}_2}$. An alternative interpretation has been given by Savin et al.[14] in terms of the local excess kinetic energy density due to the Pauli repulsion principle. This interpretation not only gives a deeper physical meaning to the ELF function but also permits generalization of ELF to any wavefunction and, in particular, to the exact one. Therefore, ELF provides a rigorous basis for the analysis of the wavefunction and of the bonding in molecules and crystals. In 1994, it was proposed to use the gradient field of ELF in order to perform a topological analysis of the molecular space[15] in the spirit of Bader's theory of atoms in molecules.[9] The attractors of ELF determine basins that are either core basin, encompassing nuclei, or valence basin, when no nucleus except a proton lies within it. The valence basins are characterized by the number of core basins with which they share a common boundary, and this number is called the valence basin synaptic order.[16] There are therefore asynaptic, monosynaptic, disynaptic, and polysynaptic valence basins. Monosynaptic basins usually correspond to lone pair regions, whereas di- and polysynaptic basins characterize chemical bonds. An advantage of this representation is that it provides a clear criterion to identify multicentric bonds. In a way, this is a complementary view to the traditional valence representation: Instead of counting bonds from a given center, which only accounts for two body links, the count is performed from the "piece of glue" that binds the atoms to one another.

From a quantitative point of view, a localization basin (core or valence) is characterized by its population (i.e., the integrated one electron density over the basin):

$$\overline{N}(\Omega_i) = \int_{\Omega_i} \rho(\mathbf{r})\, d(\mathbf{r}) \tag{1}$$

in which $\rho(\mathbf{r})$ denotes the one-electron density at $\mathbf{r}$, and Ω_i is the volume of the basin. For approximate wave functions expressed in terms of orbitals the basin population, $\overline{N}(\Omega_i)$, is the sum of orbital contributions:

$$\overline{N}(\Omega_i) = \sum_{\mu=1}^{occ.} n_\mu \langle \varphi_\mu | \varphi_\mu \rangle_{\Omega_i} \tag{2}$$

in which n_μ is the occupation number of the molecular orbital, φ_μ, labeled by μ. The orbital contributions permit examination of donation and retrodonation effects on a reliable basis.

It is also worthwhile to calculate the variance of the basin population:

$$\sigma^2(\overline{N};\Omega_i) = \int_{\Omega_i} d\mathbf{r}_1 \int_{\Omega_i} \pi(\mathbf{r}_1,\mathbf{r}_2)\, d\mathbf{r}_2 - \left[\overline{N}(\Omega_i)\right]^2 \quad (3)$$

where $\pi(\mathbf{r}_1,\mathbf{r}_2)$ is the spinless pair function.[17] Both $\overline{N}(\Omega_i)$ and $\sigma^2(\overline{N};\Omega_i)$ are observable in the sense of quantum mechanics; on the contrary, the square root of the variance, $\sigma(\overline{N};\Omega_i)$, cannot be defined by an operator and therefore its interpretation in terms of quantum-mechanical standard deviation is not fully consistent. In particular, the absolute value of $\sigma(\overline{N};\Omega_i)$ can be larger than $\overline{N}(\Omega_i)$. The relative fluctuation of the basin populations has been introduced by Bader in the case of atomic basins,[18] and its generalization to localization basins:

$$\lambda(\overline{N}_i;\Omega_i) = \frac{\sigma^2(\overline{N};\Omega_i)}{\overline{N}(\Omega_i)} \quad (4)$$

provides an indication of the delocalization within the Ω_i basin. Usually, a relative fluctuation of >0.45 is a sign of delocalization.[16] It has been shown that the variance can be readily written as a sum of contribution arising from the other basins[19]:

$$\sigma^2(\overline{N};\Omega_i) = \sum_{j\neq i} \overline{N}(\Omega_i)\overline{N}(\Omega_j) - \overline{N}(\Omega_i,\Omega_j) \quad (5)$$

In this expression, $\overline{N}(\Omega_i)\overline{N}(\Omega_j)$ is the number of electron pairs classically expected from the basin population, whereas $\overline{N}(\Omega_i,\Omega_j)$ is the actual number of pairs obtained by integration of the pair function over the basins Ω_i and Ω_j. The quantities, $\overline{N}(\Omega_i)\overline{N}(\Omega_j) - \overline{N}(\Omega_i,\Omega_j)$, calculated with the "atoms in molecules" (AIM) partition have been referred to as "topological bond orders" by Ángyán et al.[20] This definition is based on the partition of the exchange contribution to the second order density matrix independently of any variance calculation. According to Fradera et al., the term "delocalization index" is a better denomination than "topological bond order."[21] It is worth noting that this expression of the basin population variance provides a natural picture of the electron delocalization. Another interesting feature of the population analysis just outlined is that it allows one to propose valence bond resonant structures on a reliable basis.

It is also informative to consider, in addition to the basin population, the integrated spin density:

$$\langle S_z\rangle_\Omega = \frac{1}{2}\int_{\Omega_i} \left(\rho^\alpha(\mathbf{r}) - \rho^\beta(\mathbf{r})\right) d\mathbf{r} \quad (6)$$

which locates the unpaired electrons in open-shell systems as well as the pair populations:

$$\overline{N}^{\alpha\alpha}(\Omega_i,\Omega_j) = \int_{\Omega_i}\int_{\Omega_j} \Pi^{\alpha\alpha}(\mathbf{r}_1,\mathbf{r}_2)\, d\mathbf{r}_1\, d\mathbf{r}_2 \quad (7)$$

$$\overline{N}^{\alpha\beta}(\Omega_i,\Omega_j) = \int_{\Omega_i}\int_{\Omega_j} \Pi^{\alpha\beta}(\mathbf{r}_1,\mathbf{r}_2)\, d\mathbf{r}_1\, d\mathbf{r}_2 \quad (8)$$

$$\overline{N}^{\beta\beta}(\Omega_i,\Omega_j) = \int_{\Omega_i}\int_{\Omega_j} \Pi^{\beta\beta}(\mathbf{r}_1,\mathbf{r}_2)\, d\mathbf{r}_1\, d\mathbf{r}_2 \quad (9)$$

In these expressions, ρ^σ and $\Pi^{\sigma\sigma'}$ denote the spin contributions to the electron and pair densities.[17]

Computational Method

The *ab initio* calculations have been performed using GAUSSIAN-94 software.[22] The geometries of the diatomic molecules N_2, O_2, and F_2 have been optimized and the electron density calculated at the Hartree–Fock, the hybrid Hartree–Fock density functional Becke3LYP,[23–26] and the MP2 levels with the 6-31G, 6-31G*, and 6-311+G(3df) basis sets. The electron density of the polyatomic molecules, carbonohydrazide and 1,2,7,8-tetraaza-4,5,10,11-tetraoxatricyclo[6.4.1.1]tetradecane, have been calculated at the experimental geometries at the Hartree–Fock, the hybrid Hartree–Fock density functional Becke3LYP, and the MP2 levels with the 6-31G* and 6-31G** basis sets.

Results and Discussion

BASIS SETS AND CORRELATION EFFECTS: GENERAL TRENDS

The values of $\rho(\mathbf{r}_c)$, $\nabla^2\rho(\mathbf{r})_{\mathbf{r}=\mathbf{r}_c}$, and $H(\mathbf{r}_c)$ of N_2, O_2, and F_2 are presented in Table I. For the two former molecules, all criteria unambiguously conclude in covalent bonds, whereas the F_2 results are more puzzling, because the Laplacian is positive. The value of the Laplacian appears to be rather sensitive to the Coulomb correlation because the SCF method yields a value close to zero.

Table II presents the C(X), V(X), and V(X, X) basin populations for the N_2, O_2, and F_2 molecules calculated with different basis sets at the HF, Becke3LYP, and MP2 calculation levels. The number and type of basins in N_2 and O_2 do not depend upon the basis set quality or upon the correlation scheme. Both molecules show one disynaptic, V(X, X′), and two monosynaptic, V(X) and V(X′), basins. As expected from the $D_{\infty h}$ symmetry of these systems the attractors position on the C_∞ axis.

TABLE I.
Electron Density (e Å^{-3}), Electron Density Laplacian (e Å^{-5}), and Energy Density (Eh Å^{-3}) Calculated at Bond Critical Point of X_2 Molecules (X = N, O, F) with /6-311+G(3df) Basis Set.

Molecule	Method	$\rho(\mathbf{r}_c)$	$\nabla^2\rho(\mathbf{r})_{\mathbf{r}=\mathbf{r}_c}$	$H(\mathbf{r}_c)$
N_2	Becke3LYP	0.70967	–2.8130	–1.320
O_2	Becke3LYP	0.54795	–0.7562	–0.691
F_2	Becke3LYP	0.29639	0.2963	–0.300
F_2	HF	0.38370	0.0297	–0.353

TABLE II.
Basin Populations of X_2 Molecules, (X = N, O, F).[a]

Method	Basis	C(X)	V(X, X′)	V(X)
N_2				
HF	6-31G	2.1	2.8	3.5
HF	6-31G*	2.1	3.8	3.0
HF	6-311+G(3df)	2.1	3.7	3.1
Becke3LYP	6-31G	2.1	2.7	3.6
Becke3LYP	6-31G*	2.1	3.3	3.2
Becke3LYP	6-311+G(3df)	2.1	3.4	3.2
Becke3LYP	STO3G	2.1	3.5	2.9
Becke3LYP	3-21G	2.1	3.7	2.2
MP2	6-31G	2.1	2.4	3.7
MP2	6-31G*	2.1	3.2	3.3
MP2	6-311+G(3df)	2.1	3.3	3.3
O_2				
HF	6-31G	2.1	1.0	5.4
HF	6-31G*	2.1	1.4	5.2
HF	6-311+G(3df)	2.1	1.6	5.1
Becke3LYP	6-31G	2.1	0.8	5.5
Becke3LYP	6-31G*	2.1	1.2	5.3
Becke3LYP	6-311+G(3df)	2.1	1.3	5.2
MP2	6-31G	2.1	0.3	5.7
MP2	6-31G*	2.1	1.0	5.4
MP2	6-311+G(3df)	2.2	1.2	5.2
F_2				
HF	6-31G	2.1	—	6.9
HF	6-31G*	2.1	0.4	6.7
HF	6-311+G(3df)	2.1	0.5	6.6
Becke3LYP	6-31G	2.1	—	6.9
Becke3LYP	6-31G*	2.1	2 × 0.1	6.8
Becke3LYP	6-311+G(3df)	2.1	2 × 0.2	6.7
MP2	6-31G	2.1	—	6.9
MP2	6-31G*	2.13	—	6.9
MP2	6-311+G(3df)	2.1	2 × 0.1	6.7

[a] For F_2, the monosynaptic basin populations involved in the "protocovalent" bond are reported in the same column as V(X, X′).

In the case of F_2, the overall topology of the system is not structurally stable with respect to basis sets and correlation effects. In the absence of polarization functions, the three calculation schemes provide a picture in which each fluorine possesses one and only one valence basin. The addition of polarization functions induces the formation of a disynaptic basin, V(F, F′), at the Hartree–Fock level, whereas two monosynaptic basins centered on the intermolecular axis between the two cores appear in the hybrid HF/DFT and MP2 calculations [only with the 6-311+G(3df) basis set for the latter].

The core populations are always slightly larger than 2 e^-. The net effect of the polarization functions is to increase the size and therefore the population of the disynaptic basin, V(X, X′), at the expense of the monosynaptic ones. This effect is rather large especially for N_2 (i.e., in the range of 0.6 to 1.0 e^-), depending on the method of calculation. Unlike Mulliken populations, which vary in a rather nonphysical fashion upon basis set and correlation effects,[27] the behavior of basin populations is consistent with the chemical expectation that correlates the bond strength with its magnitude. Polarization functions increase the V(X, X′) populations as well as the binding energy and the stretching force constant, whereas accounting for the Coulomb correlation lowers both the basin population and the force constant. It should be noted that, in most cases, the populations are almost converged with a single set of 3d polarization functions and that there is always a satisfactory agreement between the Becke3LYP and the MP2 values.

MO VERSUS ELF

In standard MO theory, the bond orders of N_2, O_2, and F_2 are 3, 2, and 1, respectively. In principle, these numbers represent the number of electron pairs involved in the chemical bond and therefore should correspond to half of the disynaptic basin population provided by the ELF analysis. However, whatever the method of calculation, the ELF populations are much lower than the MO expectations. If one considers the antiparallel pair population calculated with eq. (8), which are 1.7, 0.65, and 0.15 for N_2, O_2, and F_2, respectively [Becke3LYP/6-311+G(3df) values] the discrepancies between the MO and the topological approach are important. As shown in Figure 1, the $3\sigma_g$ molecular orbital has two nodal surfaces, and the nonexistence of nodal planes between the nuclei indicates that the orbital is bonding.

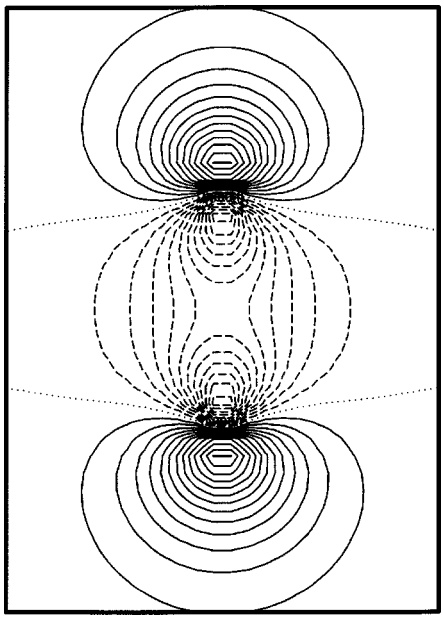

FIGURE 1. Plot of the $3\sigma_g$ molecular orbital of F_2 in a plane containing the internuclear axis. The isoline separation is 0.05. Solid, dotted, and dashed lines correspond to positive, zero, and negative values.

The relationship between molecular orbital nodal surfaces and ELF has recently been discussed in detail by Burdett et al.[28] The orbital contributions to the basin populations support this interpretation: for example, $3\sigma_g$ contributes to the V(X, X′) population for only 0.29 and 0.12 e^- in the N_2 and F_2 cases, respectively. Moreover, the basin population should be understood as arising from several Lewis resonant structures. For example, in the case of N_2, the disynaptic V(N, N′) and monosynaptic V(N) populations are consistent with a naive model in which the :N≡N: and :$\dot{\text{N}}$–$\dot{\text{N}}$: structure weights are about 0.4 and 0.6, respectively.

LOCALIZATION VERSUS DELOCALIZATION ANALYSIS

An additional support for a description in terms of resonant structures can be found in the analysis of the variance of V(X, X′) disynaptic basin populations. Such populations are presented in Table III in the case of the Becke3LYP/6-311+G(3df) calculations.

For N_2 the relative fluctuation of V(N, N′) is slightly larger than for a conventional, localized bond (i.e., 0.43 vs. 0.4; see ref. 16), the most important contributions arising from the lone pair basins V(N). As the X—X bond weakens, the relative fluctuation increases: 0.7 for O_2 and 0.84 for F_2 as well as V(X) contributions.

Other relevant data provided in Table III involve the delocalization between the lone pairs. In the case of N_2, V(N_2) contributes 30% to the V(N_1) variance; the relative contribution of V(X′) to the V(X) variance increases from N_2 to O_2 and decreases from O_2 to F_2. Such an important delocalization between lone pairs belonging to different atoms has already been identified in the case of three electron bonds—for instance, Cl_2^-, for which the topology of the ELF function shows no disynaptic basin. Therefore, a realistic description of bonding in terms of resonance structures should involve ionic structures such as X^+X^-, which ensures a delocalization between lone pair basins.

COVALENCY VERSUS PROTOCOVALENCY

The breaking of a standard covalent bond, such as in ethane, implies the splitting of the disynaptic basin through a cusp catastrophe[12] in which one attractor give rise to two attractors and one saddle point of index 1 in order to preserve the Poincaré–Hopf condition. This process occurs at an internuclear distance, the critical distance, which is usually larger than the equilibrium bond length. In many cases, there is no energy transition state and therefore the energy at the critical point is below the dissociative limit. In the case of F_2, two monosynaptic basins are found at the equilibrium distance instead of the expected disynaptic one in those calculation schemes accounting for correlation. As previously noted, correlation tends to transfer density from the V(X, X′) basin to the V(X) ones, and therefore weakens the bond with respect to Hartree–Fock (as a result, the stretching force constant calculated at the Hartree–Fock level is larger that the one calculated from DFT or post-Hartree–Fock methods). In the case of F_2, the Becke3LYP/6-311+G(3df)-optimized bond length is 1.395 Å, which is less than the experimental value of 1.435 Å and larger than the Hartree–Fock result. The electron transfer toward the lone pairs due to correlation tends to increase the bond distance, yielding to the split of the disynaptic basin. The graph of the basin populations displayed in Figure 2 clearly shows that, beyond the critical distance, $R_c = 1.325$ Å, the population of the disynaptic basin is consistently transferred toward the lone pairs. At R_c, a cusp catastrophe occurs, which splits V(F, F′) into V′(F) and V′(F′). As the bond is stretched the transfer toward the lone pairs continues until ca. 1.5 Å, a distance at which each fluorine atom

TABLE III.
X_2 Molecule (Becke3LYP/6-311+G(3df) Calculations): Basin Populations, $\bar{N}_i$, Standard Deviation, $\sigma(\bar{N}_i)$, Relative Fluctuation, $\lambda(\bar{N}_i)$, and Contributions of Other Basins (%) to $\sigma^2(\bar{N}_i)$.

Basin	$\bar{N}_i$	$\sigma(\bar{N}_i)$	$\lambda(\bar{N}_i)$	Contribution analysis
N_2				
$C(N_1)$	2.1	0.5	0.14	$V(N_1, N_2)$ 40%, $V(N_1)$ 47%, $V(N_2)$ 10%
$V(N_1)$	3.2	1.1	0.36	$V(N_1, N_2)$ 54%, $V(N_2)$ 30%,
$V(N_1, N_2)$	3.4	1.2	0.43	2 × V(N) 42%
O_2				
$C(O_1)$	2.1	0.6	0.16	$V(O_1, O_2)$ 10%, $V(O_1)$ 80%, $V(O_2)$ 9%
$V(O_1)$	5.2	1.2	0.29	$V(O_1, O_2)$ 31%, $V(O_2)$ 43%, $C(O_1)$ 23%
$V(O_1, O_2)$	1.3	0.9	0.70	2 × V(O) 46%
F_2				
$C(F_1)$	2.1	0.6	0.18	$V(F_1)$ 87%, $V(F_2)$ 10%
$V(F_1)$	6.7	0.9	0.13	$V(F_1, F_2)$ 21%, $V(F_2)$ 34%, $C(F_1)$ 43%
$V(F_1, F_2)$	0.4	0.6	0.84	2 × V(F) 47%

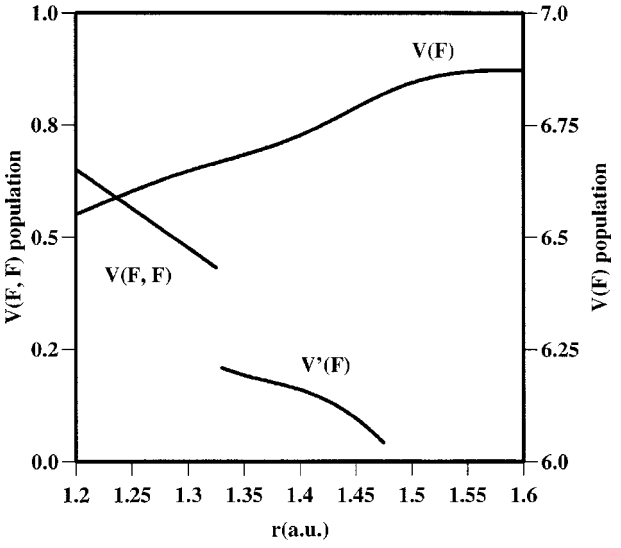

FIGURE 2. Populations of the V(F, F) and V(F) basins (in *e*) vs. the internuclear distance. At $R_c = 1.325$ Å, V(F, F) yields two basins, V(F).

bears a unique valence shell. The same behavior is followed by the N_2 molecule: beyond the critical distance (ca. 1.47 Å) the V(N, N) population decreases to 2.3, with the electrons being transferred toward the nitrogen lone pairs. It is worth noting that, at the critical distance, the V(N, N) population is close to 2 e^-, and therefore the dissociation of N_2 can be described in terms of the breaking of a single bond. Although the behavior of N_2 and F_2 are analogous, there is a large difference: in N_2, R_c is larger than the equilibrium distance, whereas in F_2 it is lower. Such a situation in which a true covalent bond, characterized by a disynaptic basin at a distance shorter than the equilibrium distance, has been previously referred to as "protocovalent." Protocovalent bonds have a low binding energy; that is, <60 kcal/mol (e.g., F_2 and H_2O_2).

BONDING IN CARBONOHYDRAZIDE AND 1,2,7,8-TETRAAZA-4,5,10,11-OXATRICYCLO [6.4.1.1]TETRADECANE

Carbonohydrazide (CH_6N_4O) and 1,2,7,8-tetraaza-4,5,10,11-tetraoxatricyclo[6.4.1.1]tetradecane ($C_6H_{12}N_4O_4$) are classical examples in which the deformation density, $\Delta\rho(\mathbf{r})$, is experimentally found to be very weak or even negative at the midpoint of some homopolar bonds.[4, 5] In the case of $C_6H_{12}N_4O_4$, Hartree–Fock calculations performed with a double-ζ (9s 5p|4s 2p)[29] basis set confirm the very weak charge accumulation observed for the N—N bonds and the depletion of the O—O single bonds.

The geometries of the CH_6N_4O and $C_4H_{12}N_4O_4$ molecules are shown in Figures 3 and 4, respectively. We maintained the atom labels given in refs. 5 and 29. Table IV presents the basin populations calculated (Becke3LYP/6-31G**) for CH_6N_4O, together with an analysis of their variance, whereas the basin populations of $C_6H_{12}N_4O_4$ are listed in Table V.

The dependence of basin populations of CH_6N_4O upon correlation effects is very small and therefore

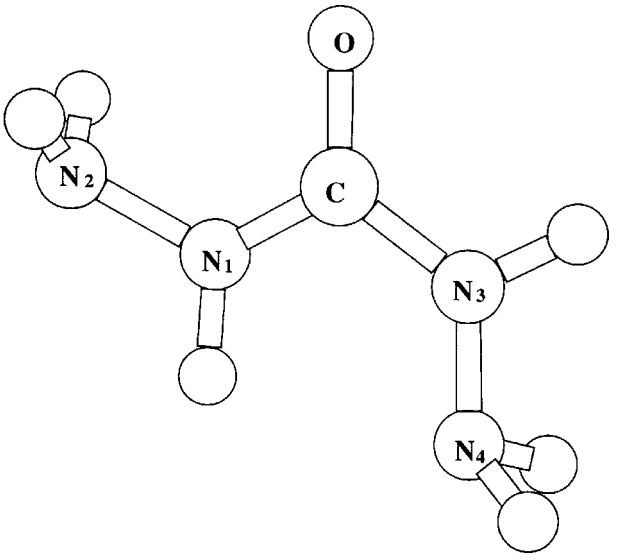

FIGURE 3. Structure and atom labels of carbonohydrazide.

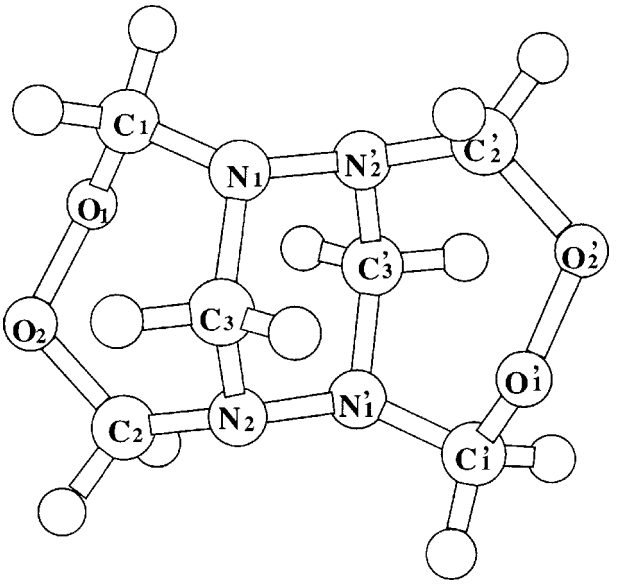

FIGURE 4. Structure and atom labels of 1,2,7,8-tetraaza-4,5,10,11-tetraoxatricyclo[6.4.1.1]tetradecane.

only Becke3LYP results are presented in Table IV. The most significant features of bonding in carbonohydrazide are the small populations of V(N, N′) and V(C, O) basins and the rather large populations of the V(C, N) ones. The conventional representation of the CO bond implies a double bond and, therefore, a population of V(C, O) of close to four. However, a rather large delocalization of the π system transfers about 1.6 e^- toward the oxygen lone pairs, which is evidenced by the large value of V(C, O) relative fluctuation (0.57) and by the large contribution of V(O) to the variance (63%). Such a low population and delocalization toward the lone pairs is also provided by the ELF analysis of formaldehyde.[30] The V(N, N′) populations are almost equal and rather low (ca. 1.3), which is consistent with the very low maximum peak height found in the experimental deformation maps. The differences between the two bonds (see Fig. 3 for atom labeling scheme) is to be found in the delocalization analysis. For both V(N_1, N_2) and V(N_3, N_4), the relative fluctuation is high and, in both cases, the delocalization implies the nitrogen lone pairs. The contributions of the terminal nitrogen monosynaptic basins are almost identical (ca. 18%), whereas the contribution of the lone pair of the carbon-linked nitrogen is larger for V(N_1), 27%, than for V(N_3), 17%. The basin population of V(N_2) is larger by 0.2 e^- than that of V(N_4), whereas V(N_3) has a remarkably small population, 1.7 e^-, due to an electronic transfer toward the V(C, N_3) disynaptic basin. On the other side of the molecule, the participation of the nitrogen lone pair in the C—N bond is less favored and the V(C, N_1) population is ca. 0.4 e^- smaller than the V(C, N_3) one. The contribution of the adjacent V(C, O) basins to the variance of the population of the two V(C, N) basins is small (<10%).

The basin populations in 1,2,7,8-tetraaza-4,5,10,11-tetraoxotricyclo(6.4.1.1)tetradecane calculated at the Becke3LYP level of correlation with the 6-31G** basis set are given in Table V. The C_i symmetry of the molecule implies three types of carbon atoms, labeled C_1, C_2, and C_3 in the study by Dunitz and Seiler, and two types of nitrogen atoms (N_1, N_2) as well as of oxygens (O_1, O_2).[4] As shown in Table V, there are almost no numerical differences between the populations of basins involving C_1 or C_2, N_1 or N_2, or O_1 or O_2. The V(C_1, O_1), V(N_1, N_2), and V(O_1, O_2) disynaptic basins appear to be electronically poor with respect to the standard Lewis picture of single bonds, whereas the populations of both V(C_1, N_1) and V(C_3, N_1) are slightly larger than two. Because the nitrogen lone pair population is also >2 (2.05), the enhancement of the V(C, N) basin populations must be due to an electronic transfer from the V(N_1, N_2) basins. In the case of the bonds involving oxygen atoms, electron transfer clearly occurs from the V(C, O) and V(O_1, O_2) disynaptic basins toward the two V(O) basins located on each of the oxygens. All these results, particularly the finding of small V(O_1, O_2) population, are consistent with experimental and standard

TABLE IV.
CON_4H_6 Molecule, Basin Populations, $\overline{N}_i$, Standard Deviation, $\sigma(\overline{N}_i)$, Relative Fluctuation, $\lambda(\overline{N}_i)$, and Contributions of Other Basins (%) to $\sigma^2(\overline{N}_i)$.

Basin	$\overline{N}_i$	$\sigma(\overline{N}_i)$	$\lambda(\overline{N}_i)$	Contribution analysis
C(O)	2.1	0.58	0.16	V(O) 77%, V(C, O) 18%
C(C)	2.1	0.50	0.12	V(O) 11%, V(C, O) 27%, V(N_1, C) 24%, V(N_3, C) 24%
C(N_1)	2.1	0.55	0.14	V(N_1, H_1) 23%, V(N_1) 36%, V(N_1, C) 21%, V(N_1, N_2) 13%
C(N_3)	2.1	0.55	0.14	V(N_3, H_4) 25%, V(N_3) 28%, V(N_3, C) 30%, V(N_3, N_4) 12%
C(N_2)	2.1	0.55	0.14	V(N_2, H_2) 27%, V(N_2, H_3) 28%, V(N_2) 34%, V(N_1, N_2) 11%
C(N_4)	2.1	0.54	0.14	V(N_4, H_5) 27%, V(N_4, H_6) 23%, V(N_4) 38%, V(N_3, N_4) 13%
V(O)	5.6	1.2	0.24	C(O) 21%, V(C, O) 61%
V(N_1)	2.2	1.1	0.58	C(N_1) 8%, V(N_1, H_1) 27%, V(N_1, C) 29%, V(N_1, N_2) 17%
V(N_3)	1.7	0.96	0.55	C(N_3) 9%, V(N_3, H_4) 26%, V(N_3, C) 31%, V(N_3, N_4) 15%
V(N_2)	2.0	0.95	0.45	C(N_2) 11%, V(N_2, H_2) 31%, V(N_2, H_3) 33%, V(N_1, N_2) 17%
V(N_4)	2.2	0.98	0.43	C(N_4) 11%, V(N_4, H_5) 30%, V(N_4, H_6) 29%, V(N_3, N_4) 17%
V(C, O)	2.1	1.1	0.58	V(O) 63%,V(N_1, C) 10%, V(N_3, C) 10%
V(C, N_1)	2.1	1.05	0.53	V(N_1) 35%, V(N_1, H_1) 12%, V(N_3, C) 12%, V(C, O) 12%
V(C, N_3)	2.5	1.12	0.5	V(N_3) 23%, V(N_3, H_4) 19%, V(N_1, C) 10%, V(C, O) 10%, V(N_3, N_4) 11%
V(N_1, N_2)	1.2	0.89	0.64	V(N_1) 27%, V(N_2) 18%, V(N_1, H_1) 9%, V(N_1, C) 9%, V(N_2, H_2) 13%, V(N_2, H_3) 14%
V(N_3, N_4)	1.2	0.89	0.64	V(N_3) 17%, V(N_4) 20%, V(N_3, H_4) 11%, V(N_3, C) 17%, V(N_4, H_5) 14%, V(N_4, H_6) 12%
V(N_1, H_1)	1.9	0.86	0.39	C(N_1) 10%, V(N_1) 48%, V(N_1, C) 18%, V(N_1, N_2) 10%
V(N_3, H_4)	1.9	0.87	0.39	C(N_3) 11%, V(N_3) 34%, V(N_3, C) 34%, V(N_3, N_4) 12%
V(N_2, H_2)	2.0	0.86	0.38	C(N_2) 10%, V(N_2) 38%, V(N_2, H_3) 31%, V(N_1, N_2) 14%
V(N_2, H_3)	2.1	0.89	0.38	C(N_2) 10%, V(N_2) 37%, V(N_2, H_2) 29%, V(N_1, N_2) 15%
V(N_4, H_5)	2.0	0.88	0.38	C(N_4) 10%, V(N_4) 38%, V(N_4, H_6) 28%, V(N_3, N_4) 15%
V(N_4, H_6)	1.8	0.85	0.4	C(N_4) 10%, V(N_4) 40%, V(N_4, H_5) 31%, V(N_3, N_4) 14%

TABLE V.
Basin Populations of 1,2,7,8-Tetraaza-4,5,10,11-Tetraoxatricyclo[6.4.1.1]Tetradecane.[a]

	Population		
Basin	Hartree–Fock	Becke3LYP	MP2
V(C_1, O_1)	1.4	1.3	1.3
V(C_2, O_2)	1.4	1.3	1.3
V(C_1, N_1)	2.0	2.0	2.0
V(C_2, N_2)	2.1	2.2	2.2
V(C_3, N_1)	1.9	1.8	1.9
V(C_3, N_2)	1.8	1.7	1.7
V(N_1, N_2')	1.3	1.3	1.2
V(O_1, O_2)	0.6	0.5	0.2
V(N_1)	2.2	2.2	2.2
V(N_2)	2.2	2.2	2.2
$V_1(O_1)$	2.4	2.5	2.5
$V_2(O_1)$	2.6	2.7	2.7
$V_1(O_2)$	2.6	2.7	2.7
$V_2(O_2)$	2.4	2.5	2.5

[a] 6-31G** calculations performed at the experimental structure. The atoms are labeled as in ref. 25.

Hartree–Fock deformation densities.[29] However, hybrid-atom deformation densities often provide a quite different description of the bonding; for example, electron density accumulation between the oxygens and density loss in the O lone pair regions.[29] With respect to the correlation schemes, the trends already observed for diatomics are verified; that is, the Coulomb correlation induces an electron transfer from bonds toward the lone pairs. Finally, Becke3LYP and MP2 yield values in close agreement.

Conclusion

Topological analysis of the ELF function is a useful tool for the characterization of covalent interaction. From a qualitative point of view, the splitting of a disynaptic basin into two monosynaptic ones upon bond stretching is the signature of the covalent bond. As shown for F_2 the critical distance at which this topological change occurs may be shorter than the equilibrium distance—in this case we propose to call such a bond "protocovalent"

rather than covalent. In the examples examined in this study, the bond strength appears to be correlated with the disynaptic basin populations, which is "common sense" in terms of chemistry. The basis set and correlation effects on basin populations can be easily explained by basic quantum-chemical reasoning. It is generally accepted that the account of electron correlation increases the bond lengths and lowers the stretching force constants, because it removes a spurious ionic component of the wave function at large internuclear separations. In other words, electron correlation usually lowers the bond strength with respect to Hartree–Fock and therefore it is expected to decrease the disynaptic basin populations. On the other hand, polarization functions that lower the molecular binding energy are expected to produce the opposite effect. This behavior is not the consequence of the instability of the basin population. On the contrary, these changes in basin populations represent strong support for their chemical significance.

The integration of the electron density over the basin yields no integers. This is not a consequence of awkward partition of the space but rather because it is a real quantity in nature (a consequence of the wave particle formulation and of the probabilistic interpretation). There is no physical reason for the bond population to be an integer number and models such as the resonance theory[31] are also consistent with this principle.

References

1. Burdett, J. K. New J Chem 1997, 21, 289.
2. Downs, J. W. J Phys Chem 1995, 99, 6849.
3. Spackman, M. A.; Maslen, E. N. Acta Cryst 1985, A41, 347.
4. Dunitz, J. D.; Sieler, P. J Am Chem Soc 1983, 105, 7056.
5. Ottersen, T.; kon Hope, H. Acta Cryst 1979, B35, 370.
6. Ottersen, T.; kon Hope, H. Acta Cryst 1979, B35, 373.
7. Ruedenberg, K.; Schwarz, W. H. E. J Chem Phys 1990, 92, 4956.
8. Coppens, P. X-Ray Charge Densities and Chemical Bonding. IUCr Texts on Crystallography; Oxford University Press: Oxford, 1997.
9. Bader, R. F. W. Atoms in Molecules: A Quantum Theory; Oxford University Press: Oxford, 1990.
10. Cremer, D.; Kraka, E. Croat Chem Acta 1984, 57, 1259.
11. Cremer, D.; Kraka, E. Angew Chem Int Ed Engl 1984, 23, 627.
12. Krokidis, X.; Noury, S.; Silvi, B. J Phys Chem A 1997, 101, 7277.
13. Becke, A. D.; Edgecombe, K. E. J Chem Phys 1990, 92, 5397.
14. Savin, A.; Jepsen, O.; Flad, J.; Andersen, O. K.; Preuss, H.; von Schnering, H. G. Angew Chem Int Ed Engl 1992, 31, 187.
15. Silvi, B.; Savin, A. Nature 1994, 371, 683.
16. Savin, A.; Silvi, B.; Colonna, F. Can J Chem 1996, 74, 1088.
17. MacWeeny, R. Methods of Molecular Quantum Mechanics; Academic: London, 1989.
18. Bader, R. F. W. In: Chalvet, O.; Daudel, R.; Diner, S.; Malrieu, J. P., eds. Localization and Delocalization in Quantum Chemistry, Vol. I; Reidel: Dordrecht, 1975, pp. 15–38.
19. Noury, S.; Colonna, F.; Savin, A.; Silvi, B. J Mol Struct 1998, 450, 59.
20. Ángyán, J. G.; Loos, M.; Mayer, I. J Phys Chem 1994, 98, 5244.
21. Fradera, X.; Austen, M. A.; Bader, R. F. W. J Phys Chem A 1998, 103, 304.
22. Frisch, M. J.; Trucks, G. W.; Schlegel, H. B.; Gill, P. M. W.; Johnson, B. G.; Robb, M. A.; Cheeseman, J. R.; Keith, T.; Petersson, G. A.; Montgomery, J. A.; Raghavachari, K.; Al-Laham, M. A.; Zakrzewski, V. G.; Ortiz, J. V.; Foresman, J. B.; Cioslowski, J.; Stefanov, B. B.; Nanayakkara, A.; Challacombe, M.; Peng, C. Y.; Ayala, P. Y.; Chen, W.; Wong, M. W.; Andres, J. L.; Replogle, E. S.; Gomperts, R.; Martin, R. L.; Fox, D. J.; Binkley, J. S.; Defrees, D. J.; Baker, J.; Stewart, J. P.; Head-Gordon, M.; Gonzalez, C.; Pople, J. A. GAUSSIAN-94, Revision D.4, Gaussian, Inc.: Pittsburgh, PA, 1995.
23. Becke, A. D. J Chem Phys 1993, 98, 5648.
24. Becke, A. D. Phys Rev 1988, A38, 3098.
25. Lee, C.; Yang, Y.; Parr, R. G. Phys Rev 1988, B37, 785.
26. Miechlich, B.; Savin, A.; Stoll, H.; Preuss, H. Chem Phys Lett 1989, 157, 200.
27. Bachrach, S. M. In: Lipkowwitz, K. B.; Boyd, D. B., eds. Reviews in Computational Chemistry; VCH: New York, 1994, pp. 171–227.
28. Burdett, J. K.; McCormick, T. A. J Phys Chem A 1998, 102, 6366.
29. Kunze, K. L.; Hall, M. B. J Am Chem Soc 1987, 109, 7617.
30. Fourré, I.; Silvi, B.; Chaquin, P.; Sevin, A. J Comput Chem. In press.
31. Pauling, L. The Nature of the Chemical Bond; Cornell University Press: Ithaca, NJ, 1948.